A98-31635

ICAS-98-5,4,1

HEAT TRANSFER MEASUREMENTS IN A ROTATING CHANNEL

T. Astarita
G. Cardone
G. M. Carlomagno

University of Naples - DETEC
P. le Tecchio, 80 - 80125
Naples, ITALY

Abstract

A new experimental methodology is used in order to perform local measurements of the heat transfer distribution nearby a 180deg sharp turn in a rotating rectangular channel by means of infrared (IR) thermography. To carry out the heat transfer measurements, the *heated-thin-foil* technique is employed and the channel is put in rotation in a vacuum tank so as to minimise the convective heat transfer losses at the outside surface of the channel. The thermal boundary condition being used during the tests is of one uniformly heated wall and three adiabatic ones. Results are reported either in local form or as averaged Nusselt number profiles along the channel. The latter representation is made in order to compare present results with the ones already existing in the literature. Local data are presented in terms of temperature and normalised Nusselt number distributions.

Introduction

It is well known that to increase the thermodynamic efficiency of gas turbine engines is necessary to increase the gas entry temperature. Present advanced gas turbines operate at gas entry temperatures much higher than metal creeping temperatures and therefore require intensive cooling of their blades especially in the early stages. A classical way to cool turbine blades is by internal forced convection: generally, the cooling air from the compressor is supplied through the hub section into the blade interior and, after flowing through a serpentine passage, is discharged at the blade trailing edge. The serpentine passage is mostly made of several adjacent straight ducts, spanwise aligned, which are connected by 180deg turns. The presence of these turns may cause modifications of the flow pattern with consequent high variations of the convective heat transfer coefficient. Furthermore the rotation of the turbine blade gives rise to Coriolis and much stronger buoyancy forces that may completely change the flow field and hence the distribution of the local heat transfer coefficient. To increase the blade life, which depends both on its temperature and on the generated thermal stresses, it is necessary to know the detailed distribution of the local convective heat transfer coefficient.

In the case of radially outward flow, the Coriolis force produces a secondary flow (in the form of a symmetric pair of secondary vortices) in the plane perpendicular to the direction of the moving fluid. The secondary flow pushes the particles in the centre of the channel towards the trailing surface, then along the latter in the direction of the sidewalls and finally back to the leading surface. With respect to the non-rotating case, the presence of these two secondary cells enhances the heat transfer near the trailing wall and reduces it at the leading surface. When the flow is reversed, i.e. radially inward flow, one has only to change the role played by the leading surface with that of the trailing one and *viceversa*. Furthermore, the heating at the walls causes a temperature difference between the core and the wall regions and between the leading and the trailing wall, so that the induced density difference and the strong centripetal acceleration due to rotation give rise to a much stronger buoyant effect. This effect magnifies the influence of the Coriolis force in the radially outward flow and reduces it in the opposite case.

The combined effects of Coriolis and buoyancy forces on the heat transfer has been investigated by many researchers; in particular, the works of Morris et al. [1,2,3], Wagner et al. [4,5], Iacovides and Launder [6], Han and Zhang [7], Mochizuki et al. [8] are acknowledged. All the previous experimental researches analyse only regionally averaged heat fluxes even though the acquired data practically agree with the assertions of the previous paragraph.

In the present work, some tests are made in the attempt to measure the maps of the heat transfer coefficient in a 180deg turn *rotating* channel by means of infrared (IR) thermography. The requirement to produce detailed and reliable local heat transfer distributions in rotating channels (including the 180deg turn) not only is important *per se* but is also relevant to validate computer programs which are often used to study these complex flows. The main objective of the

work is to use a new experimental methodology [9] which can perform measurements of the local heat transfer distribution nearby a 180deg sharp turn in a rotating rectangular channel. Another aim is to show that the use of infrared thermography in these types of problems may be advantageous because of its relatively good spatial resolution and thermal sensitivity. Moreover, the use of thermography matches both qualitative and quantitative requirements. The essential features of this methodology are [10]: it is non-intrusive; it allows a complete two-dimensional mapping of the surface to be tested; digital image processing may treat the video signal output.

Experimental apparatus

The design of the experimental apparatus (Figure 1) is a direct consequence of the *heated-thin-foil* technique [11] which is used to measure the convective heat transfer coefficient distribution, at the channel inside, by means of infrared thermography. As it will be shown later, since the external surface of the foil (which is to be viewed by the IR camera) cannot be thermally insulated, the only way to prevent high thermal losses at the channel outside is to have the channel itself rotating in a vacuum chamber. Therefore, the apparatus consists of a confinement circular tank (vacuum tank) which contains a rotating arm. The tank is 750*mm* in diameter and its structure and seals are designed to have the tank operating at an absolute pressure below 100*Pa*.

A toothed belt connects the rotating shaft to an AC electric motor which angular speed may be varied in a continuos way, in the range 0-2000*rpm*, by changing the pulleys and/or by means of an inverter. The rotating arm, which is perpendicularly mounted on the shaft, includes a two pass square channel, 34*mm* wide, 17 high (aspect ratio *AR* equal to 2) and 330*mm* long, which is balanced by a counterweight. The central partition wall between the two passes is 8*mm* thick and ends with a square tip, which is 34*mm* distant from the end wall (short side of the channel). The shaft is hollow in order to feed and to exhaust the air passing through the channel. An AR/AR Germanium window, which is placed on a hood (not shown in Figure 1) located on the side wall of the tank, is used as optical access for the IR camera.

In order to reduce the rotating weight, as well as the wall thermal conductance, both skeleton and cover of the two pass channel (Figure 2) are made of a slab of composite material (about 1*mm* thick): epoxy resin and kevlar mat. The thickness of the cover is chosen so as to have a deformation smaller than 0.1*mm* under the effect of the pressure difference between the inside of the channel and the vacuum tank. A printed circuit board, 0.4*mm* thick, is glued on the channel cover. Its conducting tracks are 5μm thick, 1.8*mm* wide, placed at 2*mm* pitch and aligned with the axes of the ducts. The printed circuit is used to generate a uniform heat flux by Joule effect and therefore is connected to a stabilised DC power source via a mercury rotating contact attached to the shaft.

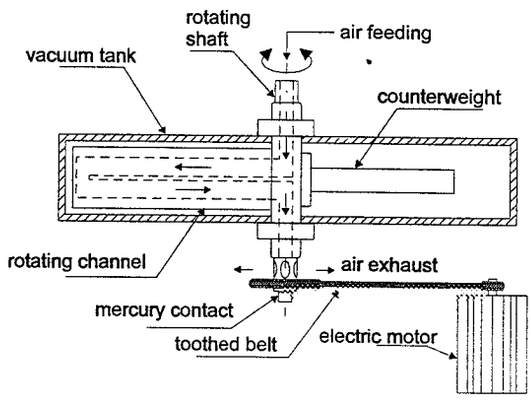

FIGURE. 1 - Experimental apparatus.

All channel walls, except for the channel cover, are thermally insulated by polyurethane slabs, 10*mm* thick, which in turn are covered by another epoxy–kevlar wall, about 1*mm* thick.

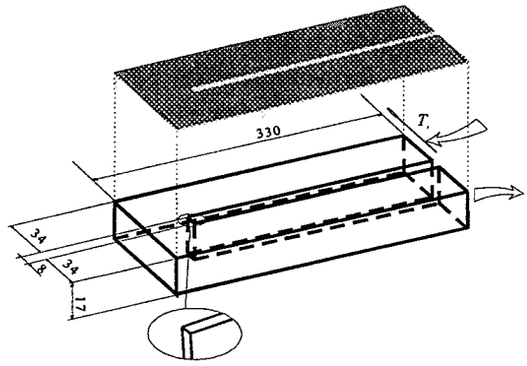

FIGURE 2. Channel skeleton and cover.

Experimental procedure

The steady state *heated-thin-foil* technique [11] is chosen to correlate the measured temperature to the local convective heat transfer coefficient *h*. In particular, for each pixel of the digitised thermal image, *h* is calculated as:

$$h = \frac{q_w - q_r}{T_w - T_b} \qquad (1)$$

where q_w is the Joule heat flux, q_r the radiative flux to ambient and channel, T_w and T_b are the wall temperature and the local bulk temperature, respectively.

Because of the low value of the pertinent Biot number, the heated wall may be considered isothermal across its thickness. The local bulk temperature T_b is evaluated by measuring the stagnation temperature of the flow T_i at the channel entrance and by making a one-dimensional energy balance along the channel, i.e. along the channel main axis; triangular heating sections are

considered in the turning zone. By measuring T_1, the temperature at the channel outlet T_2 and the air mass flow rate for each test run, an overall energy balance is also performed so as to compare the energy received by the fluid with the net electric power input.

The radiative thermal losses q_r are computed from the measured T_w and the losses due to tangential conduction are not considered.

As already mentioned before, the main problem to perform accurate measurements of the convective heat transfer coefficient, at the channel inside, is necessary to reduce the thermal losses from the surface viewed by the IR camera, i.e. at the channel outside. In the case of turbulent flow, the convective heat transfer coefficient h_c from a rotating arm to a fluid may be expressed by:

$$\frac{h_c r}{\lambda} = a\left(\frac{\rho\omega r^2}{\mu}\right)^{0.8} \qquad (2)$$

where a is a dimensionless constant, r is the radius from the axis of rotation, ω is the angular speed, ρ is the fluid density, λ and μ are the thermal conductivity and the dynamic viscosity coefficients of the fluid. Therefore, in the present case, the only way to realistically reduce the convective thermal losses is to reduce the fluid density, i.e. the air pressure in the tank.

The infrared thermographic system employed is the AGEMA Thermovision 900. The field of view (which depends on the optics focal length and on the viewing distance) is scanned by the Hg-Cd-Te detector in the 8-12μm infrared window. Nominal sensitivity, expressed in terms of noise equivalent temperature difference, is 0.07°C when the scanned object is at ambient temperature. The scanner spatial resolution is 235 instantaneous fields of view per line at 50% slit response function. During the tests a 10°x20° lens, at a viewing distance of 1.1m, is used which gives a field of view of about 0.10x0.20m^2.

The most important problem while performing this work is that, since the channel is rotating during the tests and since the frame acquisition frequency of the infrared system is 15Hz, it is not possible to take its whole thermal picture in one shot. In fact at 2000rpm, during the time necessary for the acquisition of a full frame, the channel would make more than two revolutions around its axis of rotation. It is then necessary to make use of the line scan facility of the AGEMA 900 in order to take advantage of the much higher acquisition frequency of a line (2551Hz instead of 15Hz for the full frame). Therefore, a dedicated software is developed. In particular, when the channel wall reaches thermal steady state, the acquisition of a single line at a time starts. Each time the channel passes in front of the field of view of the camera (an optical trigger connected to the main unit monitors the passage of the channel), the thermographic system *signs* the measured line. After 32 acquisitions of said line, an application software averages them and puts the averaged signal in a blank image. The procedure is automatically repeated by changing the measured line until the whole thermal image is reconstructed. Each image is digitised in a frame of 136x272 pixels at 12 bits. An application software can then perform on each thermal image: noise reduction by numerical filtering; computation of temperature and heat transfer correlations.

Results and discussion

In this section some results, in terms of temperature distributions and dimensionless convective heat transfer coefficient maps (or profiles) are presented. The temperature distributions have to be considered in terms of surface flow visualisations. Nevertheless, it has to be pointed out that, by neglecting the radiative losses and the continuous increase of T_b along the channel, the temperature difference is inversely proportional to the distribution of the convective heat transfer coefficient (see eq. 1), i.e. a higher temperature results in a lower h and *viceversa*.

In these preliminary results the effect of buoyancy is not considered so that the relevant dimensionless numbers, that rule the physical phenomena, reduce to the Reynolds number Re and the Rotation number Ro (which is the inverse of the Rossby number):

$$Re = \frac{\rho V D}{\mu} \qquad (3)$$

$$Re = \frac{\omega D}{V} \qquad (4)$$

where D is the hydraulic diameter of the channel and V is the average inlet velocity in it. The Reynolds number governs the *static* behaviour of the flow field in the channel while Ro is a dimensionless measure of the rotational effects.

The capability of thermography to perform this type of measurements is demonstrated by the three thermograms of Figure 3 which show, for Re=10000, the temperature maps of the static and rotating channel (Ro=0.14) for both the trailing side and the leading side. The thermograms show the whole channel length and are reconstructed starting from two different thermal images patched together. In this way, it is possible to increase the spatial resolution of the thermographic system. For all the three different thermograms, the rapid temperature decrease in the inlet channel is due to the development of the thermal and dynamic boundary layer.

In particular, for the non-rotating case, it is possible to notice the three high heat transfer regions, already mentioned by the present authors [12], located: just in

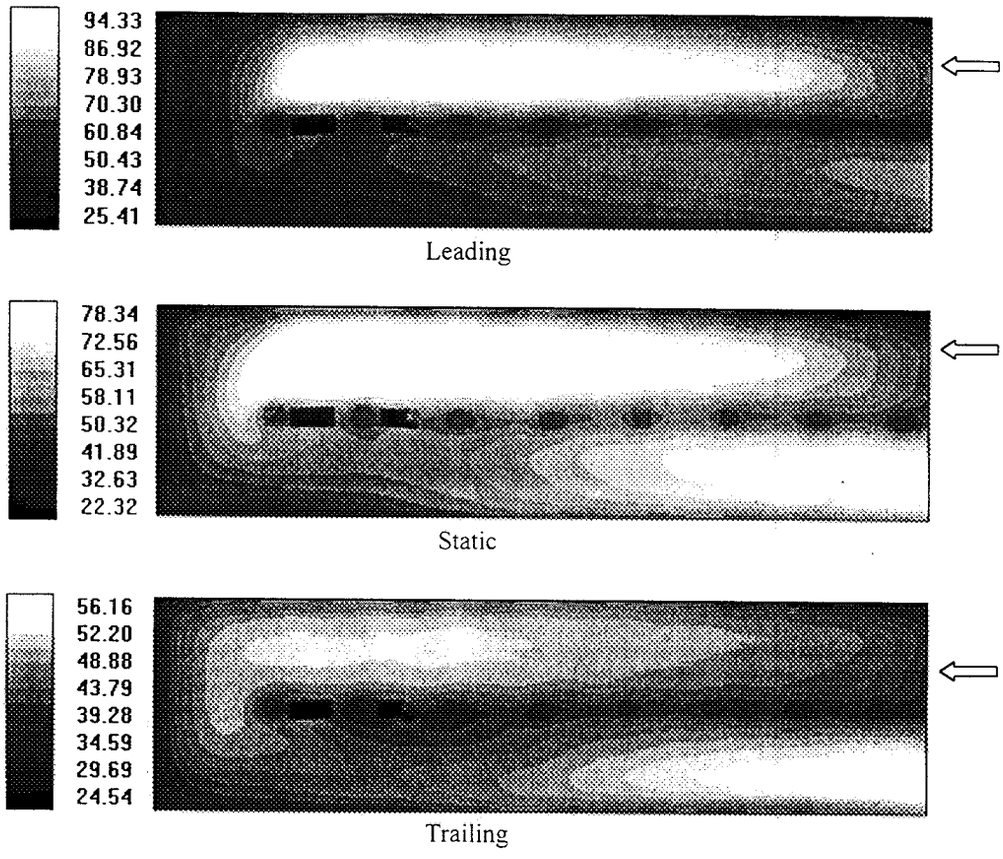

FIGURE - 3. Thermograms for the static and rotating channel: Ro=0.14; Re=10 000.

front of the inlet channel and attached to the end wall; after the second outer corner; attached to the partition wall after the bend. It is not possible to clearly distinguish the low heat transfer region already found in the first outer corner [12], both because of a lower spatial resolution of the thermal sensor and because of the different ratio between the width of the channel and that of the partition wall. While for the leading wall it is evident that the lowest heat transfer coefficient (i.e. higher temperatures) region is located in the inlet channel, for the trailing wall this region is in the outlet channel. Evidently, as stated before, the diversified behaviour for the two different sides is due to the Coriolis force effects.

In the turn zone, it is possible to see some differences between the rotating and non-rotating cases. Nearby the first outer corner the isotemperature curves seem to envisage, for the static channel, the presence of a local low heat transfer region as already found previously [12]. In the rotating case this low heat transfer zone seems to disappear especially at the leading wall. Probably this is due to a destabilisation of the low heat transfer region due to the Coriolis effects. In the second outer corner, for the leading side, the temperature distribution seems to evidence a new low heat transfer region.

The corresponding Nusselt number distributions, normalised by means of the Nusselt number Nu^* as predicted by the Dittus-Boelter correlation, are shown in Figure 4. In this case, the Nusselt distributions are relative to a lenght of three channel widths (i.e. about half of the zone of the previous thermograms). With respect to the static channel a relevant increase of the Nu values is evident at the trailing wall in the inlet channel, while the reverse is true at the leading wall. On the contrary, in the outlet channel a general decrease of Nu is noticeable at the trailing wall whereas no substantial difference occurs at the leading one. This outcome is most probably due to the effects of the buoyancy and to the secondary flow induced by the turn.

With respect to non rotating case, in the inlet channel, i.e. outward flow, it is possible to note another effect of the Coriolis forces: the Nusselt number gradient across the channel increases for the leading side and decreases for the trailing one. In fact, in the static channel, the spanwise Nusselt number variation is due either to conduction effects and to secondary flows induced by the section corners. For the trailing side the jet effect of the flow produced by the Coriolis force tends to increase the heat transfer coefficient nearby the centre of the wall reducing there the Nusselt number

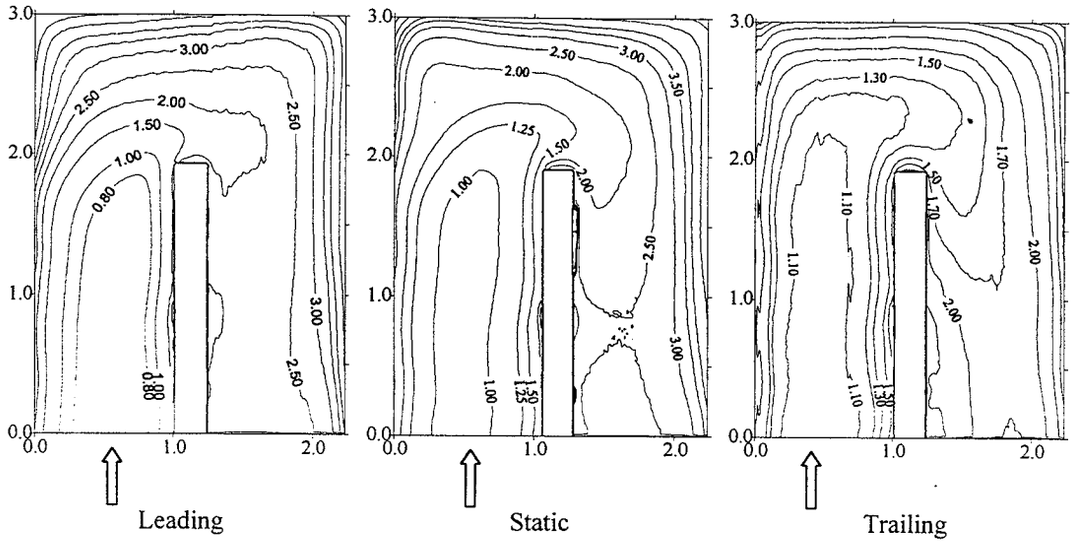

FIGURE 4 - Nusselt distribution Nu/Nu^*: Ro=0.14; Re=10 000.

gradient; the contrary occurs at the leading wall.

The maps of Figure 4 also show a different behaviour of the thermal field in the inward channel between the leading and trailing sides. In fact, while in the leading side case the position of the minimum heat transfer coefficient tends to move toward the inner wall, the reverse is true for the trailing side.

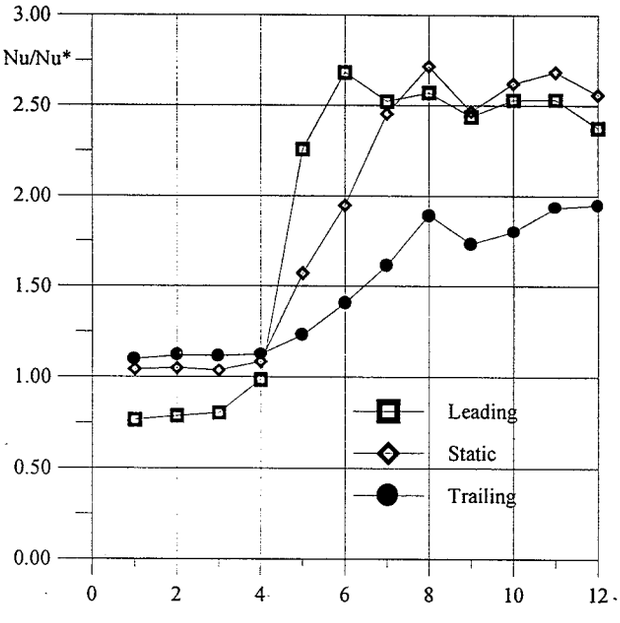

FIGURE. 5 - Segment-by-segment distribution of the average normalised Nusselt.

Figure 5 shows the segment-by-segment distribution of the spanwise averaged normalised Nusselt number; testing conditions are the same as in the previous figures. The radially outward flow corresponds to about the first four segments (1 to 4) and the radially inward to about the last four ones (9 to 12); each one of these segments is rectangular and 0.5 channel widths long. Averages in the turning zone have been made over triangular areas and the turning zone itself goes from the fifth to the eighth segment.

For the non-rotating case (Ro=0), it can be noticed that the behaviour of a fully developed flow is practically recovered up to segment 4. The higher value of Nu, with respect to Dittus-Boelter correlation, being mainly ascribed to the low Re value. Subsequently, the average Nu increases almost continuously downstream of segment 4 (at the entrance of the turn) up to segment 8 where it reaches a value about 2.5 times the one predicted by Dittus-Boelter correlation. Afterwards it must continuously decrease towards the value corresponding to a redeveloped flow.

For the rotating channel instead, the maximum Nusselt number is achieved in the turn region of the leading side. This effect, that may appear strange, can be explained taking into account the Coriolis effects. In the inward channel the Coriolis force tends to push the stream toward the trailing side but in the turn zone the component of the velocity in the radial direction suddenly decreases and then there is an inversion of the Coriolis force. This inversion can produce a separation of the flow in the inward channel, near the trailing side, and an abrupt reattachment of it toward the leading side with a strong increase of the Nusselt number at the reattachment zone. Another interesting feature is that, on the trailing wall, the secondary flow induced by the turn does not produce a very strong variation of the heat transfer coefficient.

Conclusions

A new experimental methodology is used in order to perform measurements of the local heat transfer distribution nearby a 180deg sharp turn in a rotating

rectangular channel (with an aspect ratio of two) by means of infrared thermography. To perform heat transfer measurements, the *heated-thin-foil* technique is used and the channel is put in rotation in a vacuum tank so as to minimise the convective heat transfer losses on the surface of the foil at the channel outside.

It is found that, at the trailing side of the rotating channel, the flow that is moving radially outward exhibits a higher heat transfer coefficient with respect to the non-rotating case, while the contrary is true for the leading side. Smaller differences instead are found for the inward flow. A relevant result is that in the turning zone the heat transfer coefficient is definitively higher at the leading side with respect to the trailing one.

The present results show a much better resolution of the Nusselt maps as compared to the previous ones already found the present authors [9].

Acknowledgement

The authors wish to acknowledge the financial and technical support of Alfa Romeo Avio s.p.a., Pomigliano in manufacturing the test rig.

References

1. Harasgama S. P., Morris W. D., The Influence of Rotation on the Heat Transfer Characteristics of Circular, triangular, and Square-Sectioned Coolant Passages of Gas turbine Rotor Blades, *ASME Journal of Turbomachinery*, Vol 110, pp 44-50, 1988.
2. Morris W. D., Ghavami-Nasr G., Heat transfer Measurements in Rectangular Channels With Orthogonal Mode Rotation, *ASME Journal of Turbomachinery*, Vol 113, pp 339-345, 1991.
3. Morris W. D., Salemi R., An Attempt to Uncouple the Effect of Coriolis and Buoyancy Forces Experimentally on Heat Transfer in Smooth Circular Tubes that Rotate in the Orthogonal Mode, *ASME Journal of Turbomachinery*, Vol 114, pp 858-864, 1992.
4. Wagner J. H., Johnson B. V., Hajek T. J., Heat Transfer in Rotating Passages with Smooth Walls and Radial Outward Flow, *ASME Journal of Turbomachinery*, Vol 113, pp 42-41, 1991.
5. Wagner J. H., Johnson B. V., Kopper F. C., Heat Transfer in Rotating Serpentine Passages with Smooth Walls, *ASME Journal of Turbomachinery*, Vol 113, pp 321-330, 1991.
6. Iacovides H., Launder B. E., Parametric and Numerical Study of Fully Developed Flow and Heat Transfer in Rotating Rectangular Ducts, *ASME Journal of Turbomachinery*, Vol 113, pp 331-338, 1991.
7. Han J. C., Zhang Y. M., Kalkuelhler K., Uneven Wall Temperature Effect on Local Heat Transfer in a Rotating Two-Pass Square Channel with Smooth Walls, *ASME Journal of Heat Transfer*, Vol. 114, pp. 850-858, 1993.
8. Mochizuki S., Murata A., Yang W. J., Heat Transfer Characteristics in a Rotating Square Channel with Radially Outward/inward Throughflow, Fifth International Symposium on Transport Phenomena and Dynamics of Rotating Machinery, Vol. A, may 1994, p. 398-408.
9. Astarita T. Cardone G., Carlomagno G.M., Heat Transfer Measurement in a Rotating Two-Pass Square Channel, Proc. ISROMAC-7, A. Muszynska Ed., 1664-1672, Bird Rock Publishing House, 1998.
10. Carlomagno G. M., de Luca L., Heat Transfer Measurements by means of Infrared Thermography, in *Handbook of Flow Visualization*, W.J. Yang ed., pp. 531-553 Hemisphere, 1989.
11. Carlomagno G. M., Heat Transfer Measurements by Means of Infrared Thermography, in Measurement Techniques, Von Karman Institute for Fluid Mechanics Lect. Series 1993-05, 1-114, Rhode-Saint-Genese, 1993.
12. Cardone G., Astarita T., Carlomagno G.M., Surface Flow Visualization Around a 180 deg Turn Channel for Different Aspect Ratios, Proc. VII Int. Symp. Flow Visualization, Crowder J. Ed., 977-982, Begell House Inc., New York, 1995.

Nomenclature

a	Dimensionless constant
D	Channel hydraulic Diameter
h	Heat transfer coefficient
h_e	External heat transfer coefficient
Nu	Nusselt number
Nu^*	Nusselt number as per Dittus–Boelter correlation
q_r	Radiative heat flux
q_w	Joule heat flux
r	Radius
Re	Reynolds number
Ro	Rotational number
T_1	Inlet temperature of fluid
T_2	Outlet temperature of fluid
T_b	Bulk temperature of fluid
T_w	Wall temperature of fluid
V	Fluid velocity
λ	Thermal conductivity coefficient
μ	Dynamic viscosity coefficient
ω	Angular speed
ρ	Fluid Density